

## High-Energy Neutrino Production through Photopion Processes in Blazars

C. D. Dermer<sup>1</sup> and A. Atoyan<sup>2</sup>

<sup>1</sup>Code 7653, Naval Research Laboratory, Washington, DC 20375-5352 USA

<sup>2</sup>McGill University, 3600 University Str., Montreal H3A 2T8, Canada

### Abstract.

The measured spectral energy distribution and variability time scale are used to determine the radiation and magnetic-field energy densities in the relativistic plasma that forms the gamma-ray emitting jet in the blazar 3C 279. Assuming that protons are accelerated as efficiently as electrons to a maximum energy determined by the size and magnetic field of the emitting region, we calculate the emissivity of neutrinos produced by protons that interact with the external radiation field intercepted by the jet. The external radiation field provides the most important target photons for photomeson production of high-energy neutrinos in flat spectrum radio quasars (FSRQs). Because of photomeson interactions with this field, km<sup>2</sup> neutrino telescopes are predicted to detect  $\gtrsim 0.1$ -1 neutrinos per year from blazars such as 3C 279. BL Lac objects are weaker neutrino sources if, as widely thought, their  $\gamma$ -ray emission is due to Compton-scattered synchrotron (SSC) radiation.

### 1 Introduction

Blazars are among the most powerful accelerators of relativistic particles in nature, as shown by EGRET observations of 100 MeV - GeV emission from over 60 FSRQs and BL Lac objects. Consequently, blazars represent a potential source of high-energy neutrinos (see Gaisser et al. 1995 and Halzen 2001 for reviews). The bright, highly variable  $\gamma$  radiation from blazars argues for the existence of emission regions with high photon energy densities and intense nonthermal particle populations, which are needed for efficient photomeson production (e.g., Mannheim and Biermann 1992; Mannheim et al. 2001). Previous papers have considered internal synchrotron photons as targets for high-energy proton interactions (e.g., Mannheim 1993). Here we show that UV photons from external radiation fields, which have earlier been proposed as a target photon source for nonthermal elec-

trons to produce Compton-scattered gamma-rays (e.g., Dermer and Schlickeiser 1993; Sikora et al. 1994), also provide the most important photon source for photomeson production of  $\gtrsim 30$  TeV neutrinos in FSRQs.

We use the measured spectral fluxes and variability time scales of synchrotron and Compton radiation from the blazar 3C 279 to determine physical parameters of its gamma-ray emission region. Lower limits to the Doppler factor  $\delta$  are defined by the condition that the emitting region be transparent to gamma rays. Equipartition arguments and observed fluxes of the synchrotron and Compton components are used to determine the magnetic field strength  $B$  in the plasma blob. Assuming efficient acceleration of power-law energetic protons to a maximum energy limited by the magnetic field and size scale of the region, we calculate spectral emissivities of pion decay neutrinos formed through photomeson production. Because the properties of the external radiation field are independent of the bulk Lorentz factor  $\Gamma$  of the radiating region, neutrino emissivity calculations using duty cycle estimates give accurate neutrino flux estimates during low  $\gamma$ -ray states. We predict detectable fluxes of neutrinos from  $\gamma$ -ray loud FSRQs using km<sup>2</sup> neutrino telescope arrays such as IceCube.

### 2 Constraints on Source Parameters

#### 2.1 Synchrotron and external photon energy densities

The comoving synchrotron photon energy density is given by  $u'_s \cong L_s / (2\pi r_b^2 c \delta^4)$ , where  $L_s$  is the observed bolometric synchrotron luminosity,  $r_b$  is the comoving radius of the blob, here assumed spherical, and primes denote comoving quantities. The ratio of the SSC and synchrotron luminosities  $L_{SSC}/L_s \approx u'_s/u_B$ , where  $u_B = B^2/8\pi$ . For simplicity, we consider the regime where the quasi-isotropic scattered external radiation field dominates the direct disk radiation field (Dermer and Schlickeiser 1994).

If the  $\gamma$ -rays are due to external Compton-scattered radia-

tion, then  $L_{EC}/L_s \cong \delta^2 u_{ext}/u_B \cong (\delta/\Gamma)^2 u'_{ext}/u_B$  (Sikora 1997; Dermer, Sturmer, and Schlickeiser 1997). Combining these two expressions gives  $u'_{ext}/u'_s \cong (\Gamma/\delta)^2 (L_C/L_{SSC}) \equiv a(\Gamma/\delta)^2 \cong a$  when viewing within the beam of the jet ( $\theta \lesssim \Gamma^{-1}$ ). Consequently  $u'_{ext} \cong a L_s / (2\pi r_b^2 c \delta^4)$ , where  $a \equiv L_{EC}/L_{SSC}$ . The energy of the external photons in the comoving frame is  $\epsilon'_{ext} \cong \Gamma \epsilon_{ext}$ . Models taking into account SSC and external Compton (EC) components show that a complete spectral fit requires synchrotron, SSC and EC components (Böttcher 1999; Hartman et al. 2001). Thus  $a \sim 0.1$ -1 for BL Lac objects and  $a \sim 1$ -10 for FSRQs.

The spectral energy density  $u_{ph}(\epsilon') \equiv m_e c^2 \epsilon'^2 n'_{ph}(\epsilon')$  of the photons in the blob frame is given in terms of the  $\nu F_\nu$  flux  $f(\epsilon)$  through the relation

$$u'_{ph}(\epsilon') \cong \frac{2d_L^2 f(\epsilon)}{r_b^2 c \delta^4} \cong \frac{2d_L^2 (1+z)^2 f(\epsilon)}{c^3 t_{var}^2 (d) \delta^6}. \quad (1)$$

where we relate the measured variability time scale  $t_{var}$  to the blob radius  $r_b$  through the expression  $r_b \simeq c t_{var} \delta / (1+z)$ ,  $t_{var}(d)$  is the observed variability time scale in days, and  $z$  is the redshift. The expression  $\epsilon' = \epsilon(1+z)/\delta$  relates the photon energies measured in the source and observer frames.

## 2.2 Magnetic field estimates

The magnetic field in the blob can be estimated by noting that the total soft photon energy density  $u'_{ph} = u'_s + u'_{ext} \simeq u_B (L_C/L_s)$ , where  $L_C = L_{EC} + L_{SSC}$  is the total Compton power. Hence  $u_B = (L_s/L_C) u'_{ph} = (L_s/L_C)(1+a)u'_s$ . Using the earlier expressions for  $u'_s$  and  $r_b$  gives

$$B \simeq \frac{2(1+z)\sqrt{1+a}}{c \delta^3 t_{var}} \left(\frac{L_s}{c}\right)^{1/2} \left(\frac{L_s}{L_C}\right)^{1/2}. \quad (2)$$

An independent estimate for  $B$  can also be made by introducing the equipartition parameter  $\eta = u'_{el}/u_B$  for the ratio of nonthermal electron to magnetic energy densities in the jet. Thus  $\eta \sim 1$  corresponds to equipartition, though with electrons only. For the measured synchrotron flux density  $S_\nu \propto \nu^{-\alpha_r}$  with  $\alpha_r \simeq 0.5$  at  $\nu \lesssim 10^{13}$  Hz, this gives

$$B \simeq 220 \left[ \frac{\ln(\frac{\gamma_{max}}{\gamma_{min}})}{10} \right]^{2/7} \frac{\nu_{12}^{1/7} d_{28}^{4/7} [S(Jy)]^{2/7} (1+z)^{5/7}}{\eta^{2/7} [t_{var}(d)]^{6/7} \delta^{13/7}} \quad (3)$$

in Gauss, where  $S(Jy)$  is the flux density measured at  $10^{12} \nu_{12}$  Hz.

## 2.3 $\gamma\gamma$ transparency constraints on Doppler factor

Transparency to  $\gamma\gamma$  pair-production attenuation requires that  $\tau_{\gamma\gamma}(\epsilon') \cong 2\sigma_T n'_{ph}(2/\epsilon') r_b / (3\epsilon') < 1$ , which can be rewritten as a lower limit on  $\delta$  using equation (1).

## 2.4 Photopion and neutrino production

Energy losses of relativistic protons (and neutrons) are calculated on the basis of standard expressions (see, e.g., Berezhinskii and Grigoreva 1988) for the cooling time of relativistic

protons due to photopion production in  $p\gamma$  collisions. If the ambient photons have spectral density  $n'_{ph}(\epsilon')$ , then

$$t_{p\gamma}^{-1}(\gamma_p) = \int_{\epsilon_{th}}^{\infty} d\epsilon' \frac{c n'_{ph}(\epsilon')}{2\gamma_p^2 \epsilon'^2} \int_{\epsilon_{th}}^{2\epsilon' \gamma_p} d\epsilon_r \sigma(\epsilon_r) K_{p\gamma}(\epsilon_r) \epsilon_r,$$

where  $\gamma_p$  is the proton Lorentz factor,  $\epsilon_r$  is the photon energy in the proton rest frame,  $\sigma(\epsilon_r)$  is the photopion production cross-section,  $\epsilon_{th} \approx 150$  MeV is the threshold energy for the parent photon in the proton rest frame, and  $K_{p\gamma}(\epsilon_r)$  is the inelasticity of the interaction. The latter increases from  $K_1 \approx 0.2$  at energies not very far above threshold where the single pion production channels dominate, to  $K_2 \sim 0.5 - 0.6$  at larger values of  $\epsilon_r$  where multi-pion production dominates (e.g. see Berezhinskii and Grigoreva 1988, Mücke et al. 1999).

A detailed recent study of this photohadronic process has been given by Mücke et al. (1999). In order to simplify calculations, we approximate the cross-section  $\sigma(\epsilon_r)$  as a sum of 2 step-functions  $\sigma_1(\epsilon_r)$  and  $\sigma_2(\epsilon_r)$  for the (total) single-pion and multi-pion channels, respectively, with  $\sigma_1 = 380 \mu b$  for  $200 \text{ MeV} \leq \epsilon_r \leq 500 \text{ MeV}$  and  $\sigma_1 = 0$  outside this region, whereas  $\sigma_2 = 120 \mu b$  at  $\epsilon_r \geq 500 \text{ MeV}$ . The inelasticity is approximated as  $K_{p\gamma} = K_1$  and  $K_{p\gamma} = K_2$  below and above 500 MeV. The results of our calculations in this simplified approach are found to give good agreement with earlier calculations (Berezhinskii and Grigoreva 1988). In particular, the time scales for photopion interactions of ultra-relativistic cosmic rays with the CMBR are accurately reproduced (see also Stanev et al. 2000). This approach also works well for a broad power-law distribution of field photons  $n'_{ph} \propto \epsilon'^{-\alpha_\gamma}$  for different photon spectral indices  $\alpha_\gamma$ , and readily explains the significant increase in the mean inelasticity of incident protons (or neutrons) from  $\langle K_{p\gamma} \rangle \simeq 0.2$  for steep photon spectra  $n'_{ph}(\epsilon')$  with  $\alpha_\gamma \geq 1$ , to  $\langle K_{p\gamma} \rangle \rightarrow 0.6$  for hard spectra with  $\alpha_\gamma \leq 1$  (Mücke et al. 1999).

Calculations of the spectra of secondary particles and photons ( $\nu$ ,  $\gamma$ ,  $e$ ) are done in the  $\delta$ -function approximation, assuming that the probabilities for producing pions of different charges ( $\pi^0$ ,  $\pi^+$  and  $\pi^-$ ) are equal for the multi-pion interaction channel. To correctly apply the  $\delta$ -function approximation, one has to properly take into account the different inelasticities of the multi-pion and single-pion production channels, which could explain the statement of Mücke et al. (1999) that the  $\delta$ -function approximation does not work well in the case of hard photon spectra.

## 2.5 Photon fields in the gamma-ray production region

We consider 3C 279 as a prototype FSRQ. The broad-band radiation spectra produced by the relativistic ejecta in the jet of 3C 279 is generally thought to consist of a low energy synchrotron component and high energy Compton component. In 3C 279, the synchrotron component dominates at observed frequencies  $\nu \ll 10^{16}$  Hz. We assume that the  $\nu \gg 10^{11}$  Hz synchrotron emission is cospatially located with the gamma-ray production region. This assumption is supported by observations of correlated variability between the synchrotron

and Compton components in some BL Lac objects and FS-RQs. The high-energy Compton emission consists of an SSC component and an external Compton (EC) component due to target photons that originate from outside the jet; for example from the disk, torus, scattered-disk radiation, reflected synchrotron radiation, etc.

For calculations of  $n'_{\text{ph}}(\epsilon')$  from 3C 279, we approximate the differential photon flux  $\Phi(\epsilon)$  observed during the powerful flare of 1996 (Wehrle et al. 1998) in the form of a continuous broken power-law function, with power-law photon indices  $\alpha_1 \cong 1.5$ ,  $\alpha_2 \cong 2.45$ , and  $\alpha_3 \cong 1.6$  at frequencies  $\nu \leq \nu_1 = 10^{13}$  Hz,  $\nu_1 \leq \nu \leq \nu_2 = 10^{16}$  Hz, and  $\nu \geq \nu_2$ , respectively. The  $\nu F_\nu$  energy flux  $f(\epsilon) \equiv \epsilon^2 \Phi(\epsilon)$  of the synchrotron radiation reaches a maximum value of  $1.66 \times 10^{-10}$  erg cm $^{-2}$ s $^{-1}$  at  $\nu = \nu_1$ . The maximum flux of the Compton component is  $\sim 10$  times larger than the peak synchrotron flux during the flare, and is reached at  $\sim 500$  MeV. We suppose that the SSC component makes a substantial contribution to the hard X-ray emission in 3C 279 (Hartman et al. 2001), and therefore that  $a \cong 10$ .

The redshift of 3C 279 is  $z = 0.538$ , and its luminosity distance is  $d_L(z) \cong 1.05 \times 10^{28}$  cm for an  $\Omega_m = 0.7$ ,  $\Omega_\Lambda = 0.3$  cosmology with a Hubble constant of 65 km s $^{-1}$  Mpc $^{-1}$ . The measured  $> 10^{16}$  Hz flux during the 1996 flare implies that  $\delta \gtrsim 4.9[E_{\text{ph}}(\text{GeV})^{0.117}/[t_{\text{var}}(\text{d})]^{0.19}]$  from the  $\gamma\gamma$  transparency arguments. Thus  $\delta \approx 5$  corresponds to the minimum Doppler-factor required for relativistic blobs in 3C 279 to become transparent to absorption of the observed GeV photons in the radiation field inside the blob.

Expressing  $r_b$  via the observed variability timescale  $t_{\text{var}} \sim 1$ -2 days as observed by EGRET (Wehrle et al. 1998), one finds from equation (1) that

$$u'_{\text{ph}} \sim 16 f_{-10} [t_{\text{var}}(\text{d})]^{-2} \delta_5^{-6} \text{ erg cm}^{-3}. \quad (4)$$

Here  $f_{-10} \equiv f(\epsilon)/(10^{-10} \text{ erg cm}^{-2} \text{ s}^{-1})$ , and  $\delta_5 \equiv \delta/5$ . From the observed flux of synchrotron radiation from 3C 279 with photon number index  $\alpha = 1.5$  at  $\nu \ll 10^{13}$  Hz, we deduce  $B(\text{G}) \simeq 20 \eta^{-2/7} [t_{\text{var}}(\text{d})]^{-6/7} \delta_5^{-13/7}$  from equipartition arguments. The estimation of  $B$  from equation (2) gives  $B(\text{G}) \cong 32 t_{\text{var}}^{-1}(\text{d}) \delta_5^{-3}$ , using  $L_s = 3 \times 10^{47}$  ergs s $^{-1}$ ,  $L_C/L_s \cong 10$ , and  $a \cong 10$ .

The external radiation energy density in the blob rest frame is, using the expression for  $B$  derived from equipartition arguments, given by

$$u'_{\text{ext}} \simeq 20 \left( \frac{L_{\text{EC}}}{L_s} \right) \eta^{-4/7} [t_{\text{var}}(\text{d})]^{-12/7} \delta_5^{-26/7} \text{ erg cm}^{-3}. \quad (5)$$

For the calculations we assume  $\eta = 1$  and take  $a = 10$ .

### 3 Calculations and Results

We assume that the spectrum of the external UV radiation field arises from a Shakura/Sunyaev (1973) optically-thick accretion disk model that is scattered by broad-line region clouds. This disk model has flux density  $F(\epsilon) \propto \epsilon^{1/3}$  up to a maximum photon energy  $\epsilon_{\text{max}}$  determined by the innermost

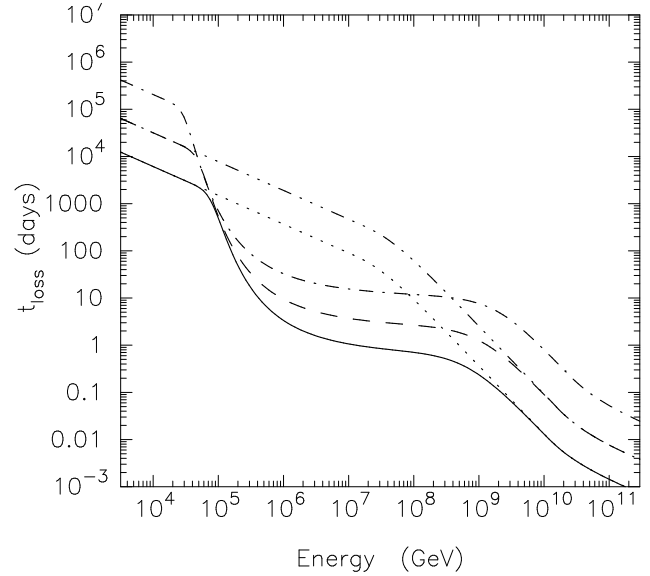


**Fig. 1.** Photomeson interaction energy loss time scale of protons, calculated for spectral fluxes observed from 3C 279 (see text) and  $t_{\text{var}} = 1$  d, assuming 3 different Doppler-factors for the jet:  $\delta = 7$  (solid curve),  $\delta = 10$  (dashed curve), and  $\delta = 15$  (dot-dashed curve). The dotted and triple-dot-dashed curves are calculated for  $\delta = 7$  and  $\delta = 10$ , respectively, when  $p\gamma$  interactions with the synchrotron radiation field alone are considered.

radius of the blackbody disk and properties of the central engine. We take  $m_e c^2 \epsilon_{\text{max}} = 35$  eV (Dermer and Schlickeiser 1993). The energy density of the external radiation in the comoving plasma blob frame can be determined by noting that  $f(\epsilon \gtrsim 1)/f(\epsilon \lesssim 1)$  corresponds to the ratio  $L_{\text{EC}}/L_s$  of the directional external Compton and synchrotron powers as measured along the jet axis.

Fig. 1 shows energy loss timescales (in the observer frame) of protons due to photopion production in a jet of 3C 279 calculated for 3 different Doppler-factors:  $\delta = 7$  (solid curve),  $\delta = 10$  (dashed curve), and  $\delta = 15$  (dot-dashed curve). The dotted and triple-dot-dashed curves show the photopion timescales corresponding to interactions with the synchrotron radiation only, for the cases  $\delta = 7$  and  $\delta = 10$ .

Fig. 2 shows the energy distributions of relativistic protons  $N_p$  in the ejecta/blobs (for the same cases as in Fig. 1), which are calculated assuming power-law injection of relativistic protons with number index  $\alpha_p = 2$  on observed timescales  $\Delta t = 2$  weeks. The total injection power of the protons  $L_p = 10^{48} \delta^{-4}$  ergs s $^{-1}$ . Note that  $10^{48}$  ergs s $^{-1}$  is the characteristic *apparent* luminosity of the flares detected by EGRET from 3C 279. In calculations of  $N_p$  we take into account the photohadron interaction energy losses, as well as the escape losses of the protons in the Bohm diffusion limit. This limit is more restrictive than the condition that the gyro-radius of the highest energies of accelerated protons should not exceed the blob size (Hillas 1984).

Fig. 3 shows the expected energy fluxes of the neutrinos produced by protons in Fig. 2. For the fluxes in Fig. 3, the

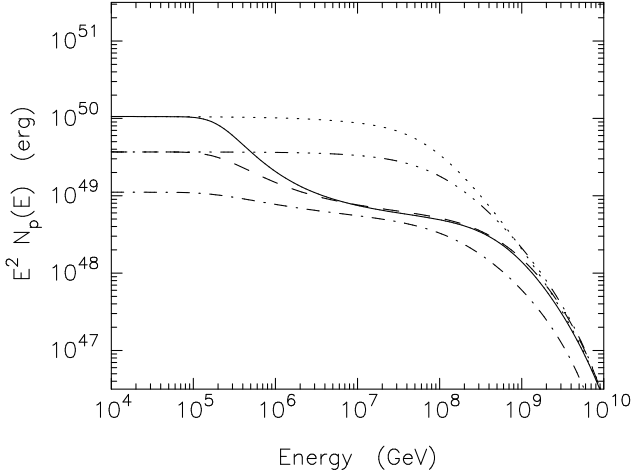


**Fig. 2.** The energy distribution of relativistic protons  $N_p$  calculated for the same jet Lorentz-factors  $\delta = 7, 10$ , and  $15$  and assumptions for the external and internal radiation fields as made in Fig. 1, assuming a power-law injection of relativistic protons with number index  $\alpha_p = 2$  during  $\Delta t = 2$  weeks with a power  $L_p = 10^{48} \delta^{-4}$  ergs  $s^{-1}$ .

total number of neutrinos that could be detected by a  $1 \text{ km}^2$  detector during 2 weeks of the flare, using neutrino detection efficiencies given by (Gaisser et al., 1995) is 0.19, 0.12 and 0.05 for the cases of  $\delta = 7, 10$  and  $15$ , respectively. It is important to note that if the external UV field is neglected, these numbers would be significantly reduced. We calculate the number of neutrinos that would be detected by a  $\text{km}^2$  array ranging from  $1.7 \times 10^{-2}$  to  $3 \times 10^{-3}$  for the fluxes in Fig. 3, which would not leave a realistic prospect for the detection of at least 2-3 neutrinos, which is required for a positive detection of a source. BL Lac objects, which have weak broad line regions and, therefore, a weak scattered external radiation field, should consequently be much weaker neutrino sources.

Because the properties of the external radiation field are insensitive to the value of the blob Lorentz factor, neutrino production in the quiescent state can be accurately estimated on the basis of properties of the external radiation field derived during the flaring state. For a typical duty factor of the flares  $\sim 1$ -2 months per year, and considering the additional neutrino production during the quiescent phase, we can reasonably expect that IceCube or other  $\text{km}^2$  array may detect several neutrinos per year from 3C 279-type blazar jets with  $\delta \lesssim 10$ . Allowing for the possibility that the nonthermal protons may have an overall power larger than that for primary electrons improves the prospects for neutrino detection.

It is important to notice that the external photon field reduces very significantly the characteristic energy of protons for effective photopion production, compared with the case of the internal synchrotron radiation field. In fact, acceleration of protons only to  $E_p \sim 10^{15} - 10^{16} \text{ eV}$  is required for efficient neutrino production through photomeson interactions, as can be seen from Fig.1. This effect permits us

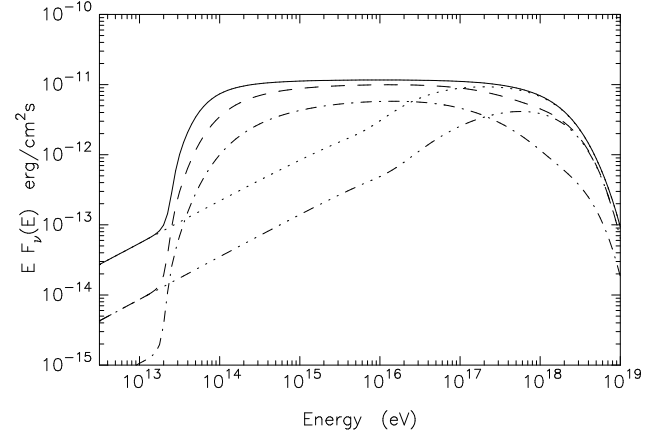


**Fig. 3.** The fluxes of neutrinos expected due to photomeson interactions of protons shown in Fig. 2 with the external (UV) and internal (synchrotron) photons in the jet of 3C 279 for Doppler factors  $\delta = 7$  (solid curve)  $\delta = 10$  (dashed curve), and  $\delta = 15$  (dot-dashed curve). The dotted and triple-dot-dashed curves show the calculated neutrino fluxes if the external photon field in the jet is neglected.

to predict that a  $\text{km}^2$  array will detect high-energy neutrinos from FSRQs without requiring acceleration of protons to ultra-high energies  $E_p \gg 10^{18} \text{ eV}$ .

## References

- Berezinskii, V. S. and Grigoreva, S. I. 1988, *Astron. Astrophys.* 199, 1
- Böttcher, M. 1999, *Astrophys. J.* 515, L21
- Dermer, C.D., and Schlickeiser, R. 1993, *Astrophys. J.* 416, 458 (DS93)
- Dermer, C.D., and Schlickeiser, R. 1994, *Astrophys. J. Suppl.* 90, 945
- Dermer, C.D., Sturmer, S.J., and Schlickeiser, R. 1997, *Astrophys. J. Suppl.* 109, 103
- Gaisser, T.K., Halzen, F., and Stanev, T. 1995, *Phys. Repts.*, 258(3), 173
- Halzen, F., 2001, in *High Energy Gamma Ray Astronomy*, ed. F.A. Aharonian and H.J. Völk (AIP: New York), p. 43
- Hartman, R.C., et al. 2001, *Astrophys. J.* in press (astro-ph/0102127)
- Hillas, A.M. 1984, *Ann. Rev. Astron. Astrophys.* 22, 425
- Mannheim, K. 1993, *Astron. Astrophys.* 269, 67
- Mannheim, K. and Biermann, P.L. 1992, *Astronomy and Astrophys.* 253, L21
- Mannheim, K., Protheroe, R.J., & Rachen, J.P. 2001, *Phys. Rev. D*, 63, 023003
- Mücke, A., Rachen, J.P., Engel, R., Protheroe, R.J., & Stanev, T. 1999, *Pub. Astron. Soc. Australia*, 16, 160
- Sikora, M., Begelman, M.C., and Rees, M.J. 1994, *Astrophys. J.* 421, 153
- Sikora, M. 1997, in the *Fourth Compton Symposium*, (AIP: New York), p. 494
- Shakura, N.I., and Sunyaev, R.A. 1973, *A&A*, 24, 337
- Stanev, T., Engel, R., Mücke, A., Protheroe, R.J., and Rachen, J.P. 2000, *Phys. Rev. D*, submitted (astro-ph/0003484)
- Wehrle, A.E., et al. 1998, *Astrophys. J.* 497, 178